Macromolecules

ARTICLE

pubs.acs.org/Macromolecules

Coarse-Grained Simulations of Penetrant Transport in Polymer Nanocomposites

Victor Pryamitsyn,* Benjamin Hanson, and Venkat Ganesan*

Department of Chemical Engineering, University of Texas at Austin, Austin, Texas 78712, United States

ABSTRACT: We report the results of coarse-grained simulations of the transport of penetrants in polymer nanocomposite materials. This work was motivated by recent experimental results in the context of conductivity and barrier properties of polymer nanocomposites. We adopt a coarse-grained simulation formalism which is suitable for studying issues surrounding the transport of ions, large gas molecules and probes in polymer nanocomposite systems. The results presented focuses on two issues: (i) the role of polymer interfacial layers and (ii) the influence of polymer matrix dynamics upon the transport properties of polymer−nanoparticle mixtures. Our results indicate that in our model the penetrant transport properties are dominated by the "filler" effect, in which the particles act as obstructions for the penetrant diffusion. Interfacial effects, which are driven by the polymer−particle interactions play a role, but their impact is shown to be less important than the filler effect. A second outcome of our work is a demonstration that matrix segmental dynamics play a very important role in determining the overall transport properties of the PNC. For nanoparticle systems, such effects are shown to lead to significant deviations from continuum mechanical theories for the effective properties of particulate dispersions.

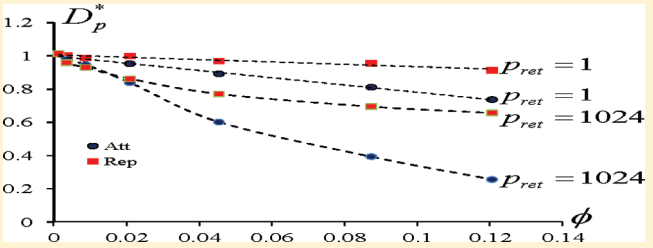

I. INTRODUCTION

Polymeric materials have been used in a variety of applications to control the transport of different permeants.[1−6] For instance, in the context of barrier and packaging materials, polymer membranes are often used to block the transport of gases such as water vapor, oxygen, CO_2, etc.[7−10] Polymer membranes have also been used in the gas separation industry, where the differences in the transport properties of gases is exploited as a means for their separation.[8,11] More recently, solid polymer electrolytes have attracted significant attention in the context of lithium ion batteries due to their abilities to transport ions of alkali metal salts.[12−15]

Adding particulate fillers (typically of the size of micrometers) to the polymer matrix to create "composites" has often been pursued as a strategy to modulate the properties of the underlying material.[16−18] Transport properties of such composites conform to the traditional view of particulate fillers, in which the latter acts as impermeable obstacles to reduce the overall transport of the penetrants. This effect, which we refer to as the "filler effect" in this article, has been the focus of many continuum mechanical models and simulations. The oldest among these models is the effective medium model of Maxwell in which the effective diffusivity D_{eff} of a composite medium containing a volume fraction ϕ of impermeable spherical particles was calculated as:[19]

$$D_{\text{eff}} = D_m \frac{1-\phi}{1+\phi/2} \tag{1}$$

where D_m denotes the diffusivity of the penetrant in the pure polymer medium. A number of researchers have followed up on the above model to use alternative theoretical approximations and/or to extend the model to treat situations involving other filler shapes, reactions within the particulate phases etc.[20−23]

In contrast to the above expectations, recent experiments have discovered that incorporating nanoscale sized fillers (termed nanoparticles and denoted as NP in this article) can in some cases *enhance* the transport over that of the pure polymer matrix. For instance, incorporating fumed silica nanoparticles or TiO_2 nanofillers in polymer membranes was shown to enhance the membrane's permeability and selectivity to large molecule penetrants.[24−29] In another related context, addition of nanosized particles of TiO_2, SiO_2, Al_2O_3 to polymer electrolytes were shown to lead to a significant increases in the conductivity of lithium ions in the material.[30−34]

A number of mechanisms have been proposed to rationalize the above observations, and a majority of them have implicated the nanoparticle-induced perturbations in the structure and dynamics of the polymer segments. Specifically, NPs have been speculated to disrupt the packing of the polymers in the polymer−particle interfacial region, causing the layers of polymer around the NPs to have higher free volume and enhanced penetrant diffusivities relative to the bulk regions.[35−39] This enhanced mobility was argued to offset and overcome the obstructional effect of the particles and lead to the enhancements noted in the transport properties. Evidence supporting such arguments were provided in the context of barrier materials through positron annihilation lifetime spectroscopy measurements which showed

Received: July 25, 2011
Revised: November 14, 2011
Published: December 01, 2011

a shift toward larger free volumes in the material with increasing NP loading.[24,25] Similar observations have also been presented in the context of mixtures of NPs with polymer electrolytes to justify the increases noted in their conductivities.[33]

Motivated by the above considerations, there have also been several theoretical investigations modeling the influence of polymer interfacial zones upon the transport properties of polymer nanocomposite (PNC) membranes. A common approach to account for filler-induced modification of polymer properties is to invoke a 3-phase model which posits the presence of three well-defined phases, viz., the particle, polymer medium and an "interfacial region" assumed to have its own physical properties.[40−44] Among these models, the recent work of Hill and co-workers[44] constitutes a comprehensive effort in which the effects of particle and penetrant sizes were incorporated within the three phase model and predictions representative of experimental results were reported. In an earlier article,[45] we extended such approaches by accounting for a continuous gradation in the properties of the interfacial layer[46−48] to elucidate the influence of polymer matrix stiffness, particle sizes and particle volume fractions upon the penetrant diffusivity properties of PNCs.

The present work and the results presented herein are motivated by two objectives:

(i) The role of polymer interfacial layers: While the above theoretical models have shed useful insights into the potential mechanisms behind the transport properties of PNCs, several issues remain unresolved. Specifically, much of the agreement reported between the models and experiments has been only at the qualitative level, and has focused on demonstrating that for appropriate choice of interfacial parameters (i.e., the size of the interfacial zones and the transport coefficients in such regions) one can potentially offset the filler effect of the particles. However, a microscopic investigation of the transport properties of the PNC matrices and a direct comparison to the results of continuum-based interfacial models has not been attempted. Such a comparison would clarify the regimes of applicability of continuum theoretical models and the parameters therein, and delineate the regimes in which NPs would actually serve to enhance the transport properties of PNC membranes.[49] Such an effort would also help shed light on the importance of alternative mechanisms which have been proposed to explain the observations noted in the context of PNC membranes and polymer electrolytes. For instance, the increases in the diffusivities of the gaseous permeants have also been ascribed to the increased void spaces created due to nanoparticle agglomeration.[26−28] In the context of polymer electrolytes, nanoparticle-induced disruption of polymer crystallization,[50] and Lewis acid−base type interactions[51] between the polymer and nanoparticles have also been advanced as factors contributing to the experimental observations. Because of the lack of quantitative models for such mechanisms, the relative importance of such features remain unresolved.

(ii) The influence of polymer segmental dynamics and temperature: This issue is motivated by the fact that in the continuum mechanical models discussed above, the influence of polymer dynamics and temperature arises only through the penetrant diffusivity values in the pure polymer matrix (quantified by the factor D_m in eq 1). However, experiments in the context of polymer electrolytes have indicated that the filler effects can exhibit a complex temperature dependence which may explicitly depend on the filler concentrations.[30,52] Motivated by these considerations, in this article we address the interplay between polymer segmental dynamics and the filler effects, and specifically the role of particle sizes in such an interplay.

In an effort to shed light on the above issues, in this work we present the results of kinetic Monte Carlo simulations of the transport properties of penetrants in polymer−nanoparticle mixtures. Our framework uses coarse-grained representations of polymer molecules, penetrants, and particulate fillers to quantify the diffusivity of penetrants as a function of the particle concentrations, polymer segmental dynamics and polymer−particle interactions. In this manner, we go beyond the above-mentioned continuum mechanical approaches, and instead directly interrogate the interfacial zone and its impact upon the overall transport properties. Moreover, by explicitly including the dynamics of polymer segments in our simulation approach, we examine the interplay between the particle interfacial effects, the filler role of the particle and the mobilities of the polymer segments.

Prior to elaborating the details of the simulation method and the results, we briefly comment on the systems which fall under the purview of the model adopted in this article. As discussed in the next section, our model invokes a linear, flexible chain representation of the polymer molecule, in which effects arising from chain rigidity and side-chain packing etc. are absent. Moreover, in the coarse-grained model that we adopt for the polymer−penetrant−particle system, the shortest units of length and time scale corresponds to that of polymer segments. Consequently, our model and results are most suited for describing penetrant motions which are either coupled to or happen at the scale of the segmental dynamics of the polymers. In this regard, we note that the dynamics of small gas molecules (such as H_2, O_2, CO_2 etc.) in glassy polymer membranes have been shown to be decoupled from the segmental motions of the polymer matrix and to be instead dependent only on the high frequency vibrational motions of the polymer chains.[53−57] Accounting for such effects in simulations requires atomistically realistic models, and will constitute the focus of a subsequent independent publication. In contrast, the motions of both larger probe molecules[58−60] as well as ions arising from alkali metal salts[61,62] have been shown to be more strongly coupled to the segmental motions of the polymer matrix. The results and analyses presented in the subsequent sections are expected to be more appropriate for the latter class of systems.

A further limitation of our study is that we examine the role of polymer−particle interactions only through its influence on the polymer densities and free volumes occurring in the interfacial layer of the particles. We note that polymer−particle interfacial interactions can also have profound consequences for the structure of the dispersion itself. In turn, the latter can have a significant effect upon the properties of the nanocomposite. Since our interest is in issues i and ii above, we restrict our attention to the macroscopic transport properties of a uniform, *randomly* dispersed suspension of nanoparticles in polymer matrices.

The rest of this article is arranged as follows: In section II, we present a brief description of the simulation methodology used in our work. In section III, we present the results of our simulations.

In section IV, we analyze the role of interfacial density perturbations. In section V, we analyze the role of polymer segmental dynamics upon the filler effects. In section VI, we summarize our findings and relate them to experimental contexts.

II. DESCRIPTION OF MODELING AND SIMULATION FRAMEWORK

A. Bond Fluctuation Model For PNCs. We used the Carmesin and Kremer version of the bond fluctuation model (BFM) for our simulations of penetrant diffusion through the PNC matrix.[63,64] In this simulation method, the monomers of the polymer are represented as cubes of sides unity which exist on a regular cubic lattice of size $L_x \times L_y \times L_z$ units. A monomer cube occupies eight lattice positions, and the excluded volume interactions between the polymer monomers are accounted by enforcing the constraint that each lattice position be occupied by utmost only one vertex of the monomer cube. The monomers are connected by bond vectors, which are chosen from within set of 108 allowed bond vectors. The resulting bond lengths are restricted to the range 2, $\sqrt{5}$, $\sqrt{6}$, 3, and $\sqrt{10}$. Elementary moves of a monomer cube takes place as jumps to the nearest neighbors along the lattice axes. The combination of the set of bond vectors and the constraints on the occupation of lattice sites ensures both self-avoidance of the monomers and prevents bond crossings. As a result, the BFM simulation approach has served as a convenient method to model both the equilibrium and dynamical properties of polymer matrices. Indeed, earlier studies have applied the BFM approach for the study of issues such as phase separation of polymer blends,[65] interdiffusion of polymers,[64] the static and dynamical properties of block copolymers[66] and the transport properties of homopolymer matrices.[67]

We model PNCs in the above framework by incorporating a coarse-grained representation of particle fillers into the BFM representation of the polymer matrix. We use the following construction to model particles in the lattice representation: A particle of radius R at location $\mathbf{R_i}$ is assumed to be comprised of the lattice cells $\{\mathbf{R}_c\}$ which are located within a distance R from the center of the particle $\mathbf{R_i}$. We start with a randomly dispersed configuration of particles and assume that the particles remain immobile. The latter assumption is expected to be reasonable since the mobility of the particles in the polymer matrices are typically very small at the temperatures of interest. The influence of polymer−particle interactions is modeled in our simulations through a short-range contact interaction between the polymer monomers and the particles. Explicitly, polymer monomers which are located a unit distance away from the particle surfaces experience an energetic gain (or loss) depending on the strength of polymer−particle interactions. To implement the latter, we consider a shell of lattice points $\mathbf{R}_0$ around the particle (whose center location is denoted as $\mathbf{R_i}$), defined such that, $R < |\mathbf{R}_0 - \mathbf{R}_i)| \leq (R + 1)$. Polymer monomers occupying this interactive shell are assumed have an energy cost of χ_p with $\chi_p \geq 0$ for repulsive polymer−particle interactions and $\chi_p < 0$ for attractive polymer−particle interactions.

The above simulation model of PNCs is used in our work to study the transport (diffusivity) properties of penetrants. To model the penetrant, we use the simplest possible representation where the penetrant is assumed to be the same size as the polymer monomer. We also assume that the penetrants behave as a "neutral solvent" with respect to both the polymer and particle components and experience no energetic interactions with either of them. Strictly speaking, such an assumption is not expected to be applicable for the description of ions and many other classes of permeants. However, to reduce the number of parameters, we adopted this simplest representation.

B. Kinetic Monte Carlo Algorithm For Transport of Penetrants. Since one of the objectives of this study was to identify the influence of polymer segmental mobilities (temperature) upon penetrant diffusivities, we assume that the time scale for motion of the penetrants can in general be different from that of polymer monomers. We choose the unit of time as the time scale for the penetrant motion and denote the time scale for polymer monomer dynamics by the parameter p_{ret}. The limit $p_{\mathrm{ret}} \lesssim 1$ corresponds to situations where the dynamics of polymer matrix is fast (relative to the penetrant motion) and is representative of the behavior of rubbery polymer matrices. In contrast, $p_{\mathrm{ret}} \gg 1$ corresponds to situations where the dynamics of polymer segments is much slower than the penetrants and is representative of the behavior of glassier polymer materials. However, we do caution that a single parameter representation may not suffice to capture all the dynamical differences between a true glassy state and a melt state. In this context, our approach is similar in spirit and validity to the idea of time temperature superposition (TTS), which has been used widely in modeling polymer properties at temperatures not too close to the glass transition temperature of the material.

To implement the above feature in our simulations, we embed the BFM simulation within a kinetic Monte Carlo framework.[68,69] Explicitly, in this approach the conventional metropolis Monte Carlo framework is modified such that the probabilities of Monte Carlo moves for the penetrant molecules and polymer monomers are chosen based on the relative time scales of their motions. More quantitatively, if we use the notation M_p to denote the total number of polymer monomers ($M_p = K_p N_p$ where N_p denotes the number of segments in the polymer chain and K_p represents the total number of polymer molecules) and N_o to denote the total number of penetrant monomers, the weighted probabilities of penetrant and polymer Monte Carlo moves W_o and W_p can be deduced as:

$$W_o = \frac{p_{ret} M_o}{p_{ret} N_o + M_p}; W_p = 1 - W_o = \frac{M_p}{p_{ret} M_o + M_p} \quad (2)$$

To implement the above, we first make a choice on whether to move the penetrant or the polymer monomer. A penetrant is chosen with a probability W_o and the polymer monomer with a probability $W_p = 1 - W_o$. Concomitantly, we add an elemental MC time step to the system clock:

$$\delta t_{MC} = \frac{p_{ret}}{p_{ret} M_o + M_p} \quad (3)$$

Next, we randomly pick up a monomer from the chosen set and attempt a BFM elementary step. The latter involves movement of the chosen moiety along one of the six lattice directions. If the target cell is unoccupied and the resulting bond lengths fall within the range of permissible BFM vectors, then the move is accepted. In the case of polymer monomers, due to the energetic interactions between the monomers and the particles, a further Metropolis criterion is used to accept or reject the move. To quantify the diffusivity of the penetrants, we probe the time dependence of the mean-squared displacement of the penetrant in the PNC

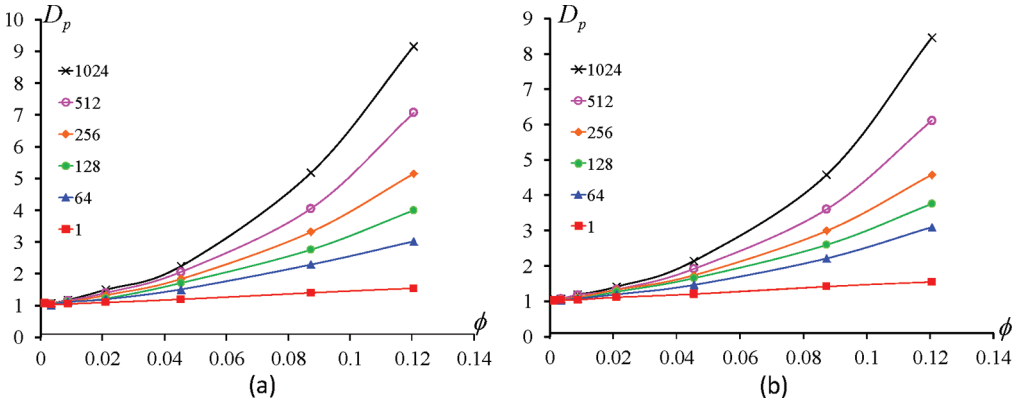

Figure 1. Penetrant diffusivities D_p (normalized to their values in the pure polymer matrix) as a function of the particle concentration ϕ. The different lines correspond to results for the p_{ret} values indicated in the legend: (a) attractive polymer−particle interactions; (b) repulsive polymer−particle interactions (lines are intended to be a guide to the eyes).

matrix and extract the long time diffusivity through the slope of its asymptotic time dependence.

C. Simulation Parameters. Our simulations are carried out in the *N*, *V*, *T* ensemble which keeps the total number of empty sites (and hence the total volume fraction of polymer and fillers) a constant upon changing the volume fraction of the particles. We fix the total occupied sites to a volume fraction of 0.5 which mimics the condition of a polymer melt for an unfilled PNC system. We note that experimental conditions are more realistically simulated using a *N*, *P*, *T* ensemble where the total number of empty sites (and the system density) may change due to the introduction of the fillers. Unfortunately, such simulations are not easily amenable with a lattice Monte carlo framework. In discussing the results, we propose a way to normalize for the density changes induced by simulation protocol and thereby probe specifically the role of interfacial layers and polymer matrix time scales.

In our simulations, we used a cubic periodical system of size 128^3 cells. The number of segments in the polymer chains was fixed as $N_p = 128$, and the total number of penetrant monomers $N_o = 60$. We set the particle size $R = 3.5$. The particle volume fractions were varied from 0.001 to 0.121 and correspondingly the number of polymer chains were varied from $K_p = 1024$ to $K_p = 777$. We studied two different polymer−filler interaction strengths corresponding to $\chi_p = 1.0$ and -1.0. $\chi_p = 1.0$ corresponds to a "repulsive" polymer−particle interaction (as confirmed by the density profiles of polymer monomers near the fillers), whereas $\chi_p = -1.0$ correspond to attractive interactions. The strength of the polymer−particle interfacial interactions are in turn expected to influence the role played by the interfacial layers upon the macroscopic diffusivities. The values chosen in our simulations, while by no means universal, are representative of the magnitudes of interactions in common filler polymer systems.[89]

The retardation factor p_{ret} was varied between 1 and 1024. $p_{ret} = 1$ can be construed as the limit (temperature) at which the segmental time scale matches with the time scale for diffusion of the penetrant. Since our model envisions the penetrant to be identical in size to the individual polymer segments (except insofar as the interactions with the particle), $p_{ret} < 1$ would be unphysical. The value $p_{ret} = 1024$ represented the upper bound for p_{ret} for which we were able to achieve statistically reliable results for penetrant diffusivity.

III. DIFFUSIVITY OF PENETRANTS IN PNC MATRICES

In parts a and b of Figure 1, we present the central results of this article, viz., the results for the diffusivity of penetrants (normalized to their values in the pure polymer matrix) in PNC matrices as functions of the volume fraction of the fillers, polymer−filler interaction strengths and polymer matrix time scales. It is seen that for both repulsive and attractive polymer−particle interactions and for all values of p_{ret} the penetrant diffusivities increases with increased particle loading. Moreover, it is seen that the polymer matrix retardation rate p_{ret} plays a significant role in determining the magnitudes of the enhancements in the penetrant diffusivities. Explicitly, it is seen that with increase in the polymer matrix time scale (i.e., at lower temperatures), the particle-induced enhancements in diffusivities become much more pronounced.

To facilitate a more closer comparison of the impact of polymer−particle interactions, in Figures 2a and b we display a comparison of the behaviors for the repulsive and attractive polymer−particle interactions for the cases of rubbery ($p_{ret} = 1$) and glassier ($p_{ret} = 1024$) polymer matrices. Surprisingly, we observe that for $p_{ret} = 1$ the particle concentration dependencies of both attractive and repulsive systems are almost identical. However, it is seen that for $p_{ret} = 1024$, the diffusivities of the attractive and repulsive systems differ from each other. These results suggest an interplay between the dynamics of the polymer matrix and the polymer−particle interactions, in a manner such that retarding the dynamics of polymer segments impact the case of attractive polymer particle systems more strongly than that of the repulsive particle systems.

Broadly speaking, the above trends which indicate an enhancement in the penetrant diffusivities with increased particle loading, are consistent with the "noncontinuum" experimental results discussed in the Introduction.[24,25,31,32] Moreover, the differences evident in the behavior of repulsive and attractive systems confirm the importance of polymer−particle interactions upon the penetrant diffusivities. However, the complex dependencies of such trends upon the polymer−particle interactions and the polymer matrix time scales suggests that the above results cannot be rationalized exclusively through considerations of filler-induced matrix structural perturbations. In the following sections, we present a quantitative analysis of the impact of particles upon the polymer structural and dynamical

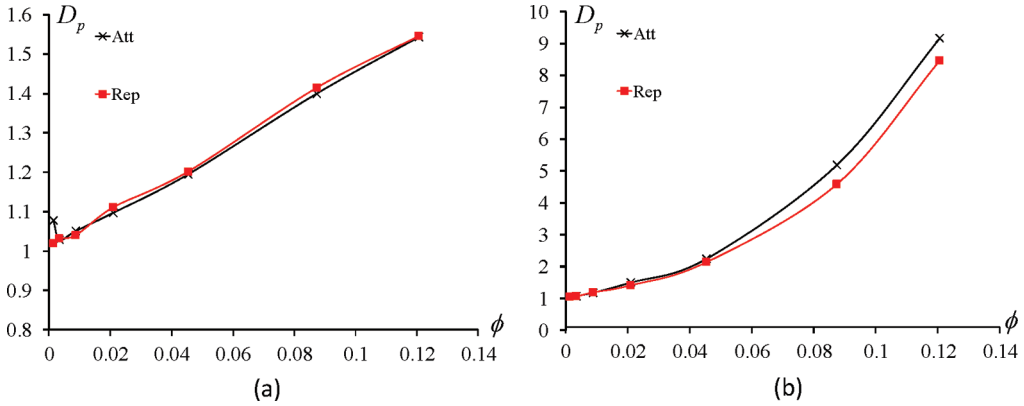

Figure 2. Comparison of the penetrant diffusivities D_p (normalized to their values in the pure polymer matrix) for attractive (Att) and repulsive (Rep) as a function of the particle concentration ϕ: (a) $p_{ret} = 1$; (b) $p_{ret} = 1024$ (lines are intended to be a guide to the eyes).

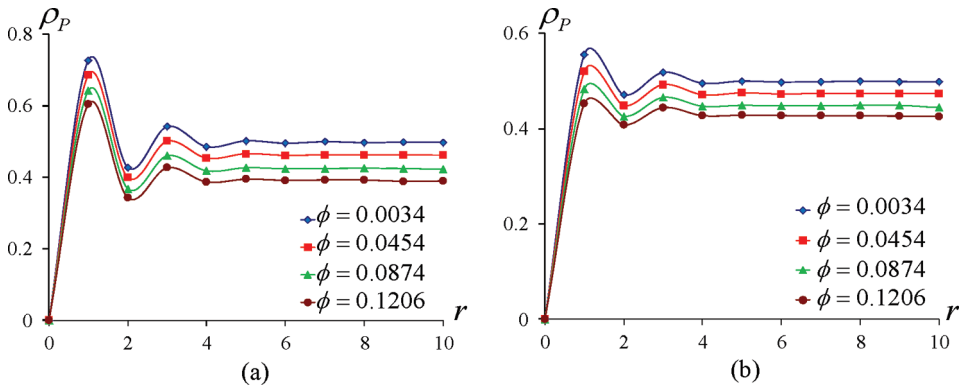

Figure 3. Density of polymer monomers as a function of the distance r from the surface of the particles for different particle loadings ϕ: (a) attractive particles and (b) repulsive particles (lines are intended to be a guide to the eyes).

characteristics to unearth the mechanisms underlying the trends noted in Figures 1 and 2.

IV. ROLE OF POLYMER MATRIX STRUCTURAL PERTURBATIONS UPON PENETRANT DIFFUSIVITIES

A. Polymer Density and Free Volume Distributions. Most prior researches have ascribed the "non-continuum" trends exhibited by the penetrant diffusivities to "interfacial" effects manifesting as particle-induced structural perturbations of the polymer matrix.[24,25,29,33] To examine the veracity of this hypothesis, in this section we present simulation results for two related quantities: (i) the local densities of polymer monomers around the particles and (ii) the void or the free volume distributions around the particle. The latter characterizes the void spaces occurring in a polymer matrix due to the packing constraints of the polymer chains and plays a prominent role in models of penetrant diffusion in polymer media.[70,71] While the distribution of free volumes are usually correlated to the density of polymers, free volumes may also embody subtle polymer chain packing effects which may not always be reflected in the local polymer densities and hence we probe these characteristics independently.

To probe the above quantities, we used a Voronois tessellation procedure to divide the space between the particles and assign different points in space to the nearest particle. Subsequently, the polymer monomer densities were averaged at each lattice point and was assigned to the nearest particle as a function of the distance of the lattice point from the particle. To quantify the distributions of free volumes in our simulations, we defined voids as the sites both (a) which are open and (b) which allow for insertion of a penetrant molecule without violation of the excluded volume constraints with surrounding polymer monomers. In the BFM approach, such sites represent the cells through which the penetrant can move through during its diffusion. Since these matrix perturbations are equilibrium characteristics, the averaged polymer densities and free volumes are independent of p_{ret}.

In parts a and b of Figure 3, we display the results for the local polymer monomer densities around the particles at different particle concentrations. The first feature we observe is the oscillations in the densities near the particle surface. These represent the "interfacial" effects which arise as a consequence of the perturbations in the polymer packing induced by the presence of the particle surfaces. Many earlier theoretical and simulations studies have focused on the origins of such features in the polymer densities and have ascribed them to an interplay between the polymer−particle interactions and the monomer−monomer correlations within the bare polymer matrix.[35,36,39,72,73] Explicitly, the polymer enhancement or depletion near the surface has been suggested to be correlated to the polymer−particle interactions, whereas the range and period of the oscillations reflects respectively the compressibility or monomer correlation lengths in the polymer matrix. Consistent with such expectations, it is seen in our results that there is a net depletion

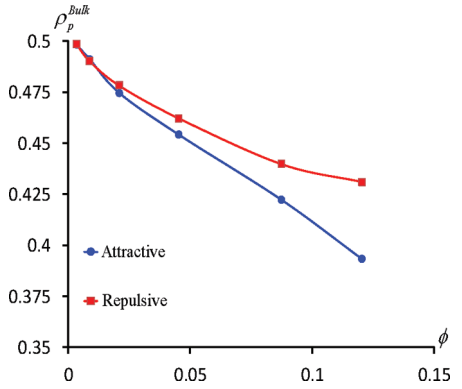

Figure 4. Comparison of the bulk densities as a function of the particle loading ϕ for the attractive and repulsive particle systems (lines are intended to be a guide to the eyes).

of polymer densities (representing the integrated densities) near repulsive particles and an enhancement of polymer densities near the particle surfaces. Moreover, the range of oscillations in the density profiles are seen to be of the order of a few monomers, which is consistent with the polymer melt-like conditions chosen for our simulations.

A second feature evident in the results of Figure 3, parts a and b, is the change in the bulk polymer densities (i.e., at far distances from the particle) as a function of the particle concentration. These bulk densities are displayed in Figure 4 wherein it can be seen that in both the attractive and repulsive particles, the bulk density is lowered with an increase in the concentration of the particles, with however a stronger effect noted for the attractive system. To rationalize these trends, we note that our simulations are performed in a constant volume ensemble where the total number of empty sites are kept a constant in the polymer−particle mixture. In such conditions, addition of particles involves concomitant removal of polymers which leads to a reduction in the overall density of polymers in the mixture. To explain the influence of polymer−particle interactions, we note that polymer densities are enhanced near the surface of attractive particles which contributes to a corresponding reduction in the bulk densities. In contrast, for repulsive particles, the polymer densities are depleted near the surface and therefore offsets (partially) the reduction in the bulk densities.

The corresponding distributions of free volume sites around the particle are displayed in Figure 5, parts a and b. In comparing the free volume profiles of with that of the monomer density distributions in Figure 3, parts a and b, it is seen that the trends displayed by the free volumes, especially their bulk values, are correlated (inversely) with the monomer density profiles. This result is physically intuitive, since regions of larger polymer density are expected to possess less space for the penetrants to move and viceversa. Consequently, the changes in the free volumes at the bulk conditions can again be rationalized as a result of our simulation protocol. However, it is also seen that the oscillations in the polymer density profiles are more pronounced compared to the trends in the free volume profiles. The latter underscores that the perturbations of free volume distributions which arise from complex polymer packing effects cannot be exclusively captured by the local values of the monomer densities. Despite such minor differences, the results of Figures 3 and 5 allow us to conclude that in our simulations, the polymer densities and free volumes are in correspondence and may be used interchangeably to identify the influence of polymer matrix perturbations upon the penetrant diffusivities.

B. Interfacial vs Filler Effects Upon Penetrant Diffusivities. On the basis of the results presented in the previous section for the density and free volume distributions, we divide the analysis of the influence of the polymer matrix structural perturbations upon penetrant diffusivities into two parts. The first contribution arises from the decrease (increase) in the overall bulk density (free volume) of the polymer (Figure 4), which would be expected to lead to an enhancement in the diffusivity of the penetrant in the bulk of the matrix. The second contribution is from the so-called "interfacial effects" representing the density and free volume perturbations near the particles. We note that it is the latter factor which has been speculated to be responsible for the noncontinuum trends observed in experiments.

We decouple the above contributions by first extracting the changes in the penetrant diffusivity arising due to changes in the bulk polymer densities. For this purpose, we probed the diffusivity of the penetrant in a pure polymer matrix as a function of polymer matrix densities for different polymer segmental time scales p_{ret}. These results are displayed in Figure 6—consistent with expectations, it is seen that the penetrant diffusivities increase with decreasing polymer density. Interestingly, it is seen that the density changes impact glassier polymers (p_{ret} = 1024) much more significantly than the case of rubbery polymers (p_{ret} = 1). Explicitly, it is seen that while the penetrant diffusivities display an almost linear retardation with increasing polymer density for p_{ret} = 1,

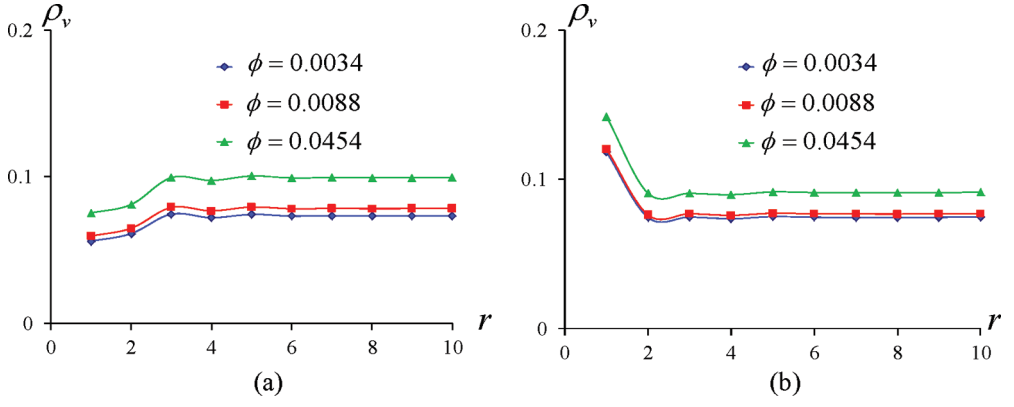

Figure 5. Free volume distributions of polymer monomers as a function of the distance *r* from the surface of the particles for different particle loadings ϕ: (a) attractive particles and (b) repulsive particles (lines are intended to be a guide to the eyes).

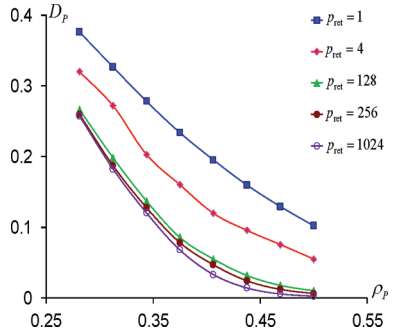

Figure 6. Penetrant diffusivities in pure polymer matrices as a function of the polymer volume fraction ρ_p and segmental time scale p_{ret} (lines are intended to be a guide to the eyes).

in contrast, for $p_{ret} = 1024$ the penetrant diffusivities approach an arrested state at higher polymer densities. In other words, the results of Figure 6 suggests that even minor changes in the bulk densities can cause significant enhancements in the penetrant diffusivities in glassier polymer matrices. In section V, we discuss the physics underlying such trends, and in section VI, we discuss possible experimental implications of this result.

To examine the specific role of the interfacial effects, we now normalize the diffusivity results of Figure 1 and Figure 2 by the diffusivity of the penetrant in the polymer matrix with however a density which corresponds to the bulk polymer density in the corresponding PNC. The so-obtained normalized penetrant diffusivity results are displayed in Figure 7, parts a and b and Figure 8, parts a and b. It is seen that in all the cases, the penetrant diffusivity *decreases* with increase in the particle concentration. A second feature which is evident in Figure 7, parts a and b, is that at small values of the retardation factor ($p_{ret} = 1$, displayed in Figure 8a), the normalized diffusivity follows a linear dependence upon the particle volume fraction. However, at larger values of polymer retardation rate ($p_{ret} = 1024$, displayed in Figure 8b), it is seen that such a simple relationship no longer holds, but instead the dependence of the particle concentration becomes much more pronounced. A third observation from the results of Figure 8, parts a and b, is that the particle concentration dependencies are much more pronounced for the case of attractive polymer−particle interactions relative to the repulsive case. Interestingly, in contrast to the results of Figures 2, parts a and b, we observe that the differences arising from the interplay between interparticle interactions and the matrix dynamics manifests even for rubbery matrices $p_{ret} = 1$ and becomes more pronounced for $p_{ret} = 1024$.

The results of Figure 7 quantify the influence of the particles and its associated interfacial layers upon the penetrant diffusivities. In this representation, the filler concentration dependence of D^*_p is seen to be qualitatively consistent with the "filler" picture of the particles in which they act as obstacles for the transport of penetrants.[20−23] By comparing the results in Figure 1 with Figure 7, we can conclude that the filler-induced enhancements noted in Figure 1 arose exclusively due to the changes in the bulk polymer density arising from the introduction of the particle fillers. More pertinent to the question raised in the introduction of this article, we observe that interfacial effects by themselves are not strong enough to overcome the "filler effects" of the particles! For instance, in the case of rubbery polymer matrices ($p_{ret} = 1$) the penetrant diffusivities are observed to follow a linear particle concentration (ϕ) dependence similar to that predicted by classical continuum mechanical theories (cf. eq 1). For glassier polymer matrices, the filler effects are more accentuated, manifesting as a pronounced lowering of the penetrant diffusivities with increased particle loadings. While polymer−particle interactions and the resulting polymer interfacial effects do play a role, the latter is seen to be less significant compared to the filler effects and manifests only as a weaker particle concentration dependence for the repulsive system in comparison to the attractive systems.

In summary, the analysis presented this section serve to establish the two central results of our simulations: (i) the enhancements in penetrant diffusivities seen in Figure 1 (or, "negative deviations" from continuum theories) arose only as a consequence the density changes in the bulk polymer conditions in the PNC; (ii) upon normalizing for the changes in the bulk densities, the overall penetrant diffusivities are dominated by the "filler" effect, in which the particles act only as obstructions for the penetrant diffusion. Interfacial effects and polymer dynamics do influence the magnitudes of penetrant diffusivities, without however changing the qualitative features of the behavior of penetrant diffusivities.

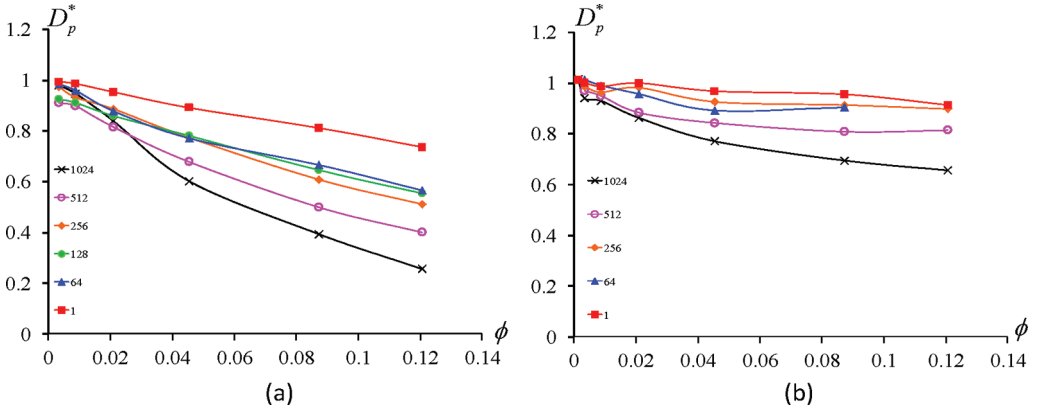

Figure 7. Penetrant diffusivities D^*_p (normalized to their values in the bulk conditions) as a function of the particle concentration ϕ. The different lines correspond to results for the p_{ret} values indicated in the legend: (a) attractive polymer−particle interactions; (b) repulsive polymer−particle interactions (lines are intended to be a guide to the eyes).

dx.doi.org/10.1021/ma201712j |*Macromolecules* 2011, 44, 9839–9851

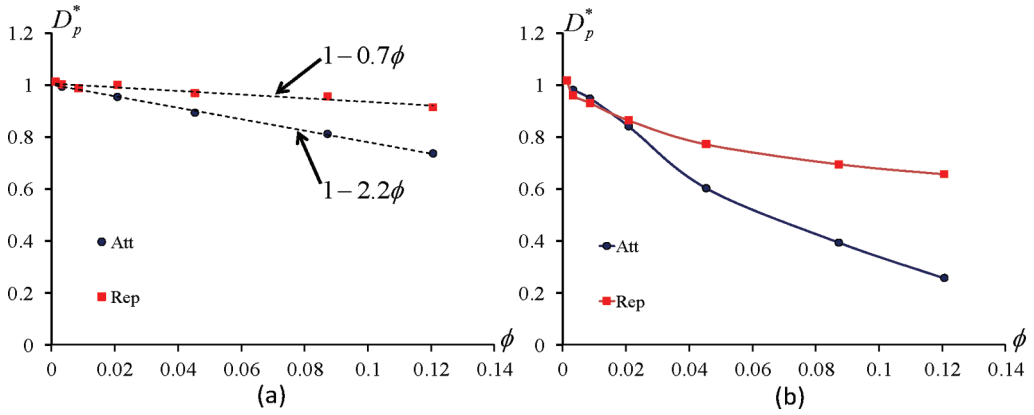

Figure 8. Comparison of the penetrant diffusivities D^*_p (normalized to their values in the bulk conditions) for attractive (Att) and repulsive (Rep) as a function of the particle concentration ϕ: (a) $p_{ret} = 1$; (b) $p_{ret} = 1024$ (lines are intended to be a guide to the eyes).

V. INFLUENCE OF POLYMER MATRIX TIME SCALES UPON PENETRANT DIFFUSIVITIES

In this section, we consider the influence of matrix segmental time scales upon filler effects. Specifically, we address the question as to why rubbery matrices exhibit a behavior close to continuum predictions (eq 1), whereas, glassier matrices seem to exhibit a much stronger influence of the particle fillers (cf. Figure 8). We address this issue at two levels: First, we consider a simple model which has been proposed in earlier studies to explain the influence of the polymer segmental time scales upon penetrant diffusivities in a pure polymer matrix. We demonstrate that the results of this model and an extension which incorporates the effect of fillers, captures the qualitative features observed in our simulation results. Subsequently, we use the physics of the model to rationalize the trends observed in our simulations. At a second level, we propose an argument which addresses the fundamental regimes of applicability of continuum mechanical models and rationalizes the p_{ret} dependent deviations of our results from such models.

A. Dynamically Disordered Random Media Model for Penetrant Diffusivities. While many models have been proposed for predicting the diffusivity characteristics of penetrants in polymer matrices, only a few of them explicitly address the role of polymer matrix time scales upon penetrant mobilities. One such model, proposed in the context of modeling ion transport in polymer membranes, is the dynamically disordered random media (DDRM) model.[74−76] In the DDRM model, the transport of penetrants through a polymer matrix is viewed (typically, within a lattice representation) as the motion of a penetrant through an array of obstacles which close and open at a regular time scale (i.e., a flickering lattice). Such a model possesses two parameters: (i) the equilibrium fraction of open sites ϕ_v, which represents the average free volume of the matrix and (ii) the time scale of opening of a closed site τ, which is directly proportional to the time scale of motion of the polymer segments. Note that the time scale of closing of an open site is determined from ϕ_v and τ through the principle of detailed balance. This model was solved analytically for the lattice case by Zwanzig and Harrison,[74] and by Nitzan, Ratner and co-workers,[75] using an effective medium approximation. While many refinements of DDRM have been proposed in subsequent studies,[76−79] in this article, we adopt the original Zwanzig−Harrison version of this model[74] as a tool to understand the role of matrix time scales and its interplay with the presence of fillers.

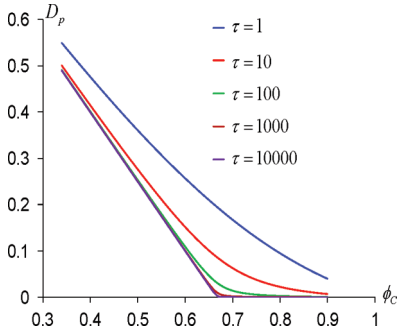

Figure 9. Predictions of the dynamical disordered random model for the penetrant diffusivities D_p as a function of the average fraction of closed sites ϕ_c for different values of time scales for opening of sites τ.

We first discuss the results of DDRM for the case when the fillers are absent. In Figure 9, we display the results of this model for the diffusivity of the penetrant (in a pure polymer matrix) as a function of the average fraction of closed sites ($\phi_c = 1 - \phi_v$) for different time scales of the polymer matrix. These results can be compared to the results displayed in Figure 6 for our penetrant diffusivities as a function of free volume and for different time scales. It is seen that there is indeed a close correspondence between the qualitative features of the two models, justifying the use of DDRM as a basis for the explanation of our simulation results.

To probe the interplay between the matrix time scales and the filler effects requires us to generalize the DDRM model to incorporate the presence of "finite" sized fillers. However, the algebraic details of such a generalization is quite involved and we defer it to a future publication, and instead, in this article we focus on a much simpler situation which involves the motion of a penetrant on a lattice which now contains a mixture of flickering sites as well as permanently immobilized lattice sites. The latter can be viewed as a model for unit sized fillers dispersed in the polymer matrix. This model has an additional parameter compared to the original DDRM model, namely the concentration of such filler sites ϕ_p. The formulas governing the generalization of DDRM model to this situation can be derived through an effective medium approximation similar to the method proposed by Nitzan and co-workers in ref 76. We summarize the pertinent

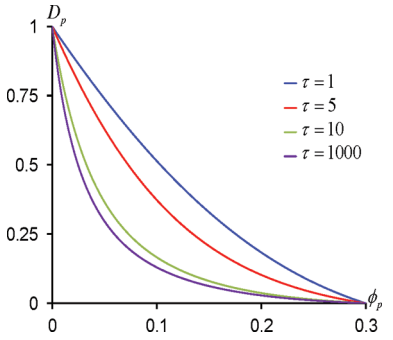

Figure 10. Predictions of the DDRM model generalized to incorporate point sized fillers. D_p denotes the penetrant diffusivity, which is depicted as a function of the filler concentration ϕ_p for different values of time scales for opening of sites τ.

formulas in Appendix and discuss the main features of its predictions below.

To mimic conditions resembling our simulations of PNCs, we fixed the concentration of the dynamically open sites (representing the polymer free volume), and probed the influence of the concentration of filler sites. These results are displayed Figure 10 for different time scales τ of the flickering sites. It is seen that for low concentrations of the particles and/or fast flickering rates ($\tau = 1$), the penetrant diffusivity is almost linear in the concentration of the particle sites. This result is consistent with our own results (Figure 7) for the rubbery matrices ($p_{ret} = 1$) and also corresponds to the trends expected from continuum models (eq 1). However, for higher concentrations of particles and/or for larger time scales τ, we observe a nonlinear dependence of the penetrant diffusivities upon the particle concentrations. The latter is qualitatively similar to the trends observed in our simulation results for glassier polymer conditions (cf. Figure 8b).

Since the qualitative features of the DDRM model are in excellent agreement with our simulation results, we can use the DDRM model to provide a physical basis for the matrix time scale dependence of penetrant diffusivities noted in our simulations. Preliminary to such an effort, we first explain the physics underlying the results of Figure 9 (and Figure 6). The extreme cases of $\phi_c \simeq 0$ or $\tau \leq 1$ are the easiest to understand. When $\phi_c \simeq 0$, there is a large enough fraction of open sites that the penetrant is able to find some pathway for diffusion even if one or more of the adjoining sites are blocked. In the other situation, when $\tau \ll 1$, closed sites surrounding the penetrant open up on a fast enough time scale to allow for the penetrant diffusion. In both the preceding situations, the penetrant motion is practically unaffected by the dynamics of the matrix, and the penetrant mobility is explicitly proportional to $\phi_v (= 1 - \phi_c)$ through the reduced concentration of the average number of open sites. For the more interesting regime when the time scale for opening (and closing) is such that $\tau \gg 1$, the penetrant gets trapped in clusters of open sites surrounded by closed sites. In the extreme case of a frozen matrix ($\tau = \infty$), the motion of the penetrant can only occur through a connected path of open sites. Since such paths cease to exist below the percolation threshold of open sites, the penetrant mobility also drops to zero below the percolation threshold. For the case of a finite but large τ, the closed sites around the penetrant can eventually open up (on the time scale τ) to facilitate the motion of the penetrant. In this regime, the penetrant mobility becomes significantly hindered and is extremely sensitive to the interplay between statistics of open site clusters (which in turn depends on the average fraction of open sites ϕ_v) and the time scale τ, and hence exhibits a nonlinear dependence on ϕ_v.

Using the above observations, we can now rationalize the matrix time-scale dependent behaviors observed in Figure 7 and 10. From the above discussion, it is evident that for $\tau \lesssim 1$, penetrant diffusion is not impacted by the dynamical phenomena of the matrix and is reduced only due to the lower concentration of the open sites. In such situations, introduction of a dilute concentration ϕ_p of particle fillers (with ϕ_c maintained dilute enough such that ϕ_v does not become too small), only reduces the concentration of the open sites. Consequently, the mobility of the penetrants are reduced by a factor proportional to ϕ_p. These considerations are consistent with the linear particle concentration dependencies observed in our simulations for the penetrant diffusivities in rubbery matrices.

For glassier matrices ($\tau \gg 1$), the discussion in the context of pure matrix suggests that the penetrant diffusion in the polymer matrix happens through clusters of open sites which become few and far apart. Upon the introducing particle fillers into the matrix, the fillers break up these clusters of open sites due to their function as permanently immobilized sites. Overall, this leads to a retardation of the penetrant diffusion, albeit, in a nonlinear manner due to the dependence of the latter on the resulting cluster distribution of open sites. In this regard, repulsive particles can be expected behave differently and have a less pronounced effect compared to attractive particles because of the reduction in polymer density occurring near the surfaces of the particle. This can be expected to open up some sites near the particles which facilitate penetrant diffusion and thereby partially offset the filler effect.

B. Noncontinuum Behavior and Interplay of Filler, Matrix Time Scale Effects. In this section, we discuss the physics underlying the interplay between the filler role of the particles and the matrix time scale effects. As noted in the Introduction, continuum mechanical theories subsume the role of the latter as just one that determines the bare penetrant diffusivity. However, our simulation results (and the correspondence to the DDRM) demonstrate that the matrix time scale could couple nontrivially with the filler effects. In this section, we propose a scaling parameter which quantifies the role of matrix time scale in influencing the filler effects.

We begin this discussion by considering the manner in which the characteristics of penetrant motion depend on the matrix time scales p_{ret}. Specifically, with increasing p_{ret}, the penetrant motion in the polymer matrix is expected to resemble the motion of a probe in a glassier medium. Prior simulations have demonstrated that for such situations,[54,80−83] the probe motion displays anamolous diffusion characteristics at short time and length scales. Such features are most conveniently captured in the "non-Gaussian" parameter $\alpha(t)$ defined as[84−86]

$$\alpha(t) = \frac{3}{5}\frac{\langle r^4(t)\rangle}{\langle r^2(t)\rangle^2} - 1$$

which quantifies the deviations of the fourth moment of displacement ($\langle r^4(t)\rangle$) of a tagged tracer from the value expected based on normal, Gaussian distribution of displacements. Nonzero values of $\alpha(t)$ correspond to deviations from the "normal" diffusion behavior.

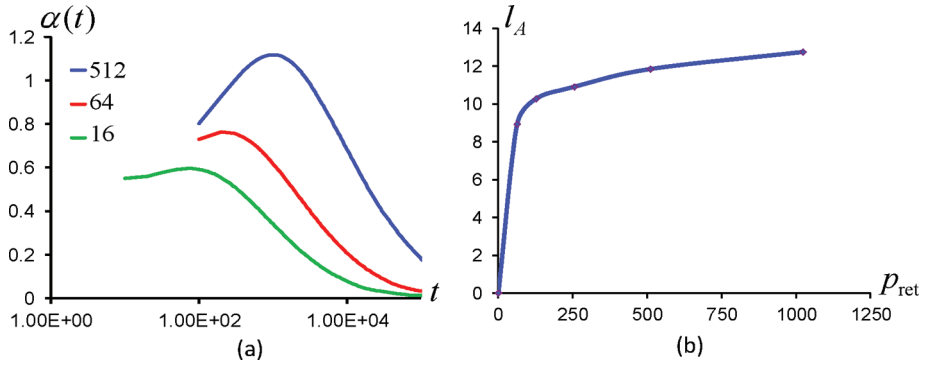

Figure 11. (a) Time-dependence of the non-Gaussian parameter $\alpha(t)$ for penetrant motion in the pure polymer matrix for different values of p_{ret} indicated in the legend; (b) Length scale characterizing the regime of anamolous diffusion l_A displayed as a function of the polymer segmental time scale p_{ret} (lines are intended to be a guide to the eyes).

In parts a and b of Figure 11, we display $\alpha(t)$ for the penetrant motion in our simulations. It can be seen that $\alpha(t)$ initially increases and reaches a maximum and then decays to zero at long times, confirming the anamolous nature of diffusion of the penetrant. This behavior can be rationalized by noting that for glassier polymer conditions, the motion of the penetrants consists of two regimes: (i) motion within small clusters of open sites which are surrounded by the (dynamically) immobile polymer segments; followed by (ii) longer time diffusive motion of the penetrant due to the diffusion of the open sites themselves (facilitated by the movement of the polymer segments). As the polymer segments become slower (larger p_{ret}), the penetrants are trapped for longer times, which leads to accentuated anamolous diffusion characteristics.

We quantify the above characteristics by extracting a length scale over which the penetrant diffusion remains anamolous. A precise definition of the latter is not necessary for the qualitative arguments we propose below, and hence we use the width of $\alpha(t)$ as a parametric function of the mean-squared displacement of the penetrant as a characteristic length scale l_A quantifying the anamolous diffusion characteristics. In other words, we define

$$l_A = \left[\frac{\int_0^\infty r^2\alpha(r^2)}{\int_0^\infty \alpha(r^2)}\right]^{1/2} \quad (4)$$

where $\alpha(r^2)$ denotes the function $\alpha(t)$ expressed parametrically as a function of the mean-squared displaced $r^2(t)$. Shown in Figure 11b are the so-determined l_A, displayed as a function of the p_{ret}. Consistent with the explanations above, we observe that increasing the matrix time scales leads to an increase in the length scale over which anamolous diffusion persists.

The above considerations pertain to the case of a penetrant diffusing in a pure polymer matrix. Upon introduction of the fillers, a new length scale characterizing the geometry of the particle suspension arises. A convenient measure for the latter is the "average pore diameter," which we denote as l_P and is defined as the average distance of an arbitrary point in a suspension to the nearest point on the solid surface.[87,88] The latter has been widely employed in the analysis of diffusion problems in porous media and analytical expressions quantifying the particle concentration dependence of l_p have been furnished for hard sphere suspensions. For this work, we used eqs 2.17−2.26 of Torquato and Avellaneda.[87]

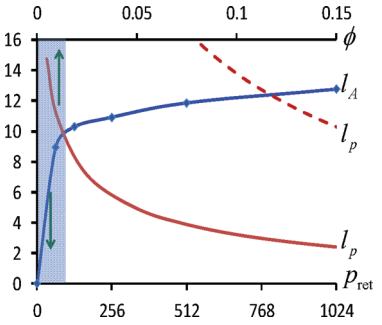

Figure 12. Comparison of the length scale of anamolous diffusion (denoted l_A, indexed to the primary X axis) with the average pore diameter (denoted l_p, indexed to the secondary X axis). The solid line for l_p was computed for a particle radius of 3.5 which corresponds to our simulation parameters. The shaded region corresponds to the regime where continuum predictions are expected to hold. The dotted line represents l_p for a hypothetical system with a particle radius of 15 units, in which the continuum regime (not displayed) is considerably expanded (lines for l_A are intended to be a guide to the eyes).

Our argument for the p_{ret} dependent deviations from the continuum models seen in our simulations is as follows: Continuum approaches such as Maxwell model (and others similar in spirit) are based on the picture of the penetrant exhibiting "normal" diffusion behavior on the scale of the particle suspension l_p. However, in the case of diffusion of penetrants in glassier polymer matrices, our discussion above establishes an additional length scale, l_A, over which the diffusion is anamolous. We propose that if $l_A \ll l_P$, then the diffusion process of the penetrant on the scale of the PNC suspension is "normal" and continuum mechanical considerations can be expected to hold. In contrast, when $l_A \gg l_P$, the diffusion process of the penetrant is no longer normal on the scale of the particle suspension and deviations from continuum mechanical predictions become manifest.

We provide evidence for the above proposal in Figure 12, by comparing the length scales l_p and l_A for different particle concentrations and matrix time scales p_{ret}. Consistent with intuitive expectations, the pore size diameter is seen to decrease with increasing particle concentration. We note that only in the regime of small p_{ret} and dilute particle concentrations, the inequality $l_p > l_A$ holds. This result is consistent with the agreement with continuum predictions noted in our simulation results for $p_{ret} = 1$. In contrast, we observe that for larger p_{ret}, $l_A \gg l_p$

which rationalizes the deviations noted from continuum predictions.

We emphasize that the above postulated breakdown of continuum predictions manifests mainly in the *nanoscopic* filler regime. Indeed, since the length scale l_p is directly proportional to the radius of the particle R (the only length scale in the particle suspension)[87] increasing R leads to a corresponding increase in l_p. Beyond a certain radius of the filler, this would render $l_p > l_A$ for all reasonable values of p_{ret} and particle volume fractions ϕ (cf. dotted lines in Figure 12 for a fictitious scenario in which the particle size is $R = 15$ units). In such situations, we would expect the continuum predictions to hold and that the matrix time scale would only serve to determine the bare penetrant diffusivities. Conversely, moving to a smaller particle radius R would lead to deviations from continuum models becoming manifest at even smaller p_{ret}. In other words, the polymer matrix time scale (temperature) determines the radius beyond which a particle may be considered to be a "macroscopic" filler for the modeling of transport properties!

In summary, we suggest that the ratio l_p/l_A determines the interplay between matrix time scale and the filler effects. For systems involving low matrix free volumes (such as our simulation conditions), penetrant diffusion is anamolous on length scales comparable to and even larger than the pore scale of the filler suspension. The latter leads to strong deviations from the continuum predictions in the form of a nonlinear dependence of penetrant diffusivity upon the particle concentration. These findings demonstrate that continuum mechanical theories and models which ignore the role of matrix time scales (except as a factor which normalizes the bare penetrant diffusivity) may prove inadequate for the modeling of transport properties of PNC membranes.

VI. SUMMARY AND EXPERIMENTAL IMPLICATIONS

In summary, we used BFM simulations to understand the mechanistic origins of penetrant diffusion in PNC materials. For this purpose, we used the simplest possible model of a monomeric penetrant diffusing through a model well-dispersed PNC matrix. Because of the coarse-grained nature of the model (the smallest length scale of the phenomena which can be captured corresponds to the polymer segments), our results are more likely applicable to penetrants of size scale comparable or larger than the scale of polymer segments. The latter class includes ions of solid alkhali metals, large gas molecules, and dye probes. In this final section, we briefly comment on the important outcomes of our analysis and their correspondence to experimental conditions.

(i). Interfacial vs Filler Effects. The overall penetrant diffusivities were then shown to be dominated by the "filler" effect, in which the particles act only as obstructions for the penetrant diffusion. While interfacial effects driven by polymer−particle interactions were shown to play a role and explain the differences between attractive and repulsive particle systems, the physical range of such perturbations were small in the polymer melt systems and hence their impact upon the penetrant diffusivity was shown to be less important relative to the "filler" effect. The overall content of this result is in disagreement with a majority of the proposals advanced to explain the filler-induced *enhancements* in the transport properties of polymer membranes.

In seeking to address the generality of the above conclusions, it is useful to recall some of the limitations of our model. We recall that our model is based on the use of a homogeneous, random dispersion to mimic the structure of the nanoparticles in the polymer matrix. However, it is well-known that polymer−particle interactions can play a significant role in influencing the structure, and in-turn the properties, of the composite.[35−37,73] For instance, aggregation of particles may lead to overlap of interfacial layers, which may open up a percolating pathway for the diffusing penetrant.

A second limitation was that we examined only a narrow range of parameters for quantifying the strengths of the polymer−particle interactions. It may be speculated that larger polymer−particle interaction strengths may change the overall transport properties of the interfacial layer and thereby accentuate its impact. Finally, our results are for the case of a model of a "neutral" solvent. Polymer-penetrant and particle-penetrant interactions may also influence the transport properties of the penetrant. Relaxing some or all of these assumptions, may potentially change the quantitative role of the interfacial layers upon the transport properties of the composite.

(ii). Importance of Changes in the Bulk Conditions of Free Volumes and Densities. Our simulation results did exhibit *enhanced* penetrant diffusivities with the addition of nanoparticles. We attributed such trends to the implementation of the simulation protocol and the resulting particle-induced density and free volume changes in the bulk polymer conditions in the PNC. Moreover, since our results indicated that for the case of glassier polymer matrices, the penetrant diffusivities are sensitive to small density and free volume changes, even minor changes to the bulk conditions may suffice to exert a significant influence upon the overall penetrant diffusivities.

We note that there are at least three experimentally realizable situations wherein nanoparticle-induced property changes may influence the transport of penetrants: (a) If the polymer matrix is crystallizable and if addition of particles disrupt the crystallization of the polymer,[50] then we would expect that the bulk density to be lower compared to that of the pure polymer matrix. This would endow a higher mobility for the ions in the bulk and rationalize the enhancements in the conductivities noted in experiments. (b) Polymer membranes and polymer−nanoparticle mixtures which are prepared deep in the glassy regime usually do not achieve equilibrium,[26−28] and are accompanied by a very slow aging process which evolves the system toward equilibrium. Such nonequilibrium effects become even more important for rigid polymers and in aggregating filler systems which are commonly used in barrier applications. In such situations, we expect the bulk densities and free volume conditions to be lower than that of the pure polymer matrix, and contribute to filler-induced enhancements noted in the experiments. (iii) Addition of fillers would likely change the thermal expansivity of the matrix and may render the bulk densities and free volumes to be a function of particle loading and temperature.

(iii). Importance of Matrix Mobilities (and Temperature). An important outcome of our analysis is the conclusion that the matrix dynamics plays a very important role in determining the overall transport properties of the PNC. This happens in a 2-fold way: On the one hand, as discussed above, the matrix time scales govern the sensitivity of the penetrant diffusivities to the bulk free volume and density changes. Whence changes in transport properties arising due to changes in bulk conditions are intimately tied to the matrix dynamics. On the other hand, our results and analysis of section V demonstrated that there is an interplay between the matrix time scales and the "filler" effects.

For nanoparticle systems, such effects were shown to lead to significant deviations from continuum mechanical theories. Overall, these results demonstrate that polymer matrix dynamics need to be explicitly accounted in any consideration of transport properties of PNC membranes.

In summary, our conclusions shed important light on the physical origins of the properties of PNCs and their modeling. Admittedly, the above conclusions were derived using a simple coarse-grained model which does not possess the detail of an atomistically realistic model. Extensions of the present work aimed at examining the influence of the size of penetrants, the impact of polymer-penetrant interactions, and the role of polymer crystallization will constitute directions for future study. Furthermore, in a followup article, we will present results from atomistically based simulations which more closely mimic the conditions required to simulate the transport of small gas molecules through polymer matrices and demonstrate that many of the qualitative features of the above conclusions also hold for such systems.

APPENDIX A: DYNAMICAL DISORDERED RANDOM MEDIA MODEL

In this appendix, we quote the pertinent results of the generalized DDRM model used for generating the results of Figures 9 and 10. These formulas can be derived straightforwardly using the effective medium theory approach proposed in ref 76.

We denote the fraction of filler sites by the symbol ϕ_p and the average number of closed flickering sites by the symbol ϕ_c. The time scale governing the flickering sites is denoted as τ. The average free volume (or open sites) of the system is denoted as ϕ_v and is given as:

$$\phi_v = 1 - \phi_c - \phi_p \tag{A1}$$

The long time mobility of the penetrant D_p in a lattice with the above parameters is then obtained as the solution of an implicit equation:

$$D_p = \frac{\phi_v - p_c(1-\chi)(1-\varepsilon g(\varepsilon))}{1 - p_c(1-\varepsilon g(\varepsilon))} - \frac{\chi p_c}{1-p_c} \tag{A2}$$

where

$$\chi = \frac{\phi_p \phi_v}{1-\phi_p}; \quad \varepsilon = \frac{1-\phi_p}{\tau D_p} \tag{A3}$$

and $p_c = {}^1/_3$ corresponding to the percolation threshold for a static, simple cubic lattice. The function $g(\varepsilon)$ represents the lattice Green's function, and has been tabulated for a number of lattices and dimensions in the Appendix E of ref 76.

AUTHOR INFORMATION

Corresponding Author

*E-mail: (V.P.) victor@che.utexas.edu; (V.G.) venkat@che.utexas.edu.

ACKNOWLEDGMENT

This work was supported in part by a grant from Robert A. Welch Foundation (Grant F1599), the US Army Research Office under Grant W911NF-07-1-0268 and National Science Foundation (DMR 1005739). We acknowledge the insightful comments and suggestions of Profs. Timothy Lodge, Mark Ediger, John Torkelson, Igal Szleifer, Kenneth Schweizer and Sanat Kumar based on a preliminary version of the results presented at the Telluride Polymer Physics Meeting, 2011. We also thank Prof. Thomas Truskett for discussions relating to the statistical geometry of suspensions.

REFERENCES

(1) Barrer, R. M. *J. Polym. Sci.* **1957**, *23*, 315.
(2) Barrer *J. Polym. Sci.* **1957**, *23*, 331.
(3) Baker, R. W.; Wijmans, J. G.; Kaschemekat, J. H. *J. Membr. Sci.* **1998**, *151*, 55–62.
(4) Aoki, T. *Prog. Polym. Sci.* **1999**, *24*, 951–993.
(5) Sangaj, N. S.; Malshe, V. C. *Prog. Org. Coat.* **2004**, *50*, 28–39.
(6) Koros, W. J.; Fleming, G. K. *J. Membr. Sci.* **1993**, *83*, 1–80.
(7) Frisch, H. L. *Polym. Eng. Sci.* **1980**, *20*, 2–13.
(8) Stern, S. A.; Frisch, H. L. *Annu. Rev. Mater. Sci.* **1981**, *11*, 523–550.
(9) Jonquieres, A.; Clement, R.; Lochon, P. *Prog. Polym. Sci.* **2002**, *27*, 1803–1877.
(10) Auras, R.; Harte, B.; Selke, S. *Macromol. Biosci.* **2004**, *4*, 835–864.
(11) Robeson, L. M. *J. Membr. Sci.* **1991**, *62*, 165–185.
(12) Berthier, C.; Gorecki, W.; Minier, M.; Armand, M. B.; Chabagno, J. M.; Rigaud, P. *Solid State Ionics* **1983**, *11*, 91–95.
(13) Armand, M. *Solid State Ionics* **1983**, *9−10*, 745–754.
(14) Bruce, P. G.; Vincent, C. A. *J. Chem. Soc., Faraday Trans.* **1993**, *89*, 3187–3203.
(15) Tarascon, J. M.; Armand, M. *Nature* **2001**, *414*, 359–367.
(16) Weston, J. E.; Steele, B. C. H. *Solid State Ionics* **1982**, *7*, 75–79.
(17) Capuano, F.; Croce, F.; Scrosati, B. *J. Electrochem. Soc.* **1991**, *138*, 1918–1922.
(18) Choudalakis, G.; Gotsis, A. D. *Eur. Polym. J.* **2009**, *45*, 967–984.
(19) Choy, T. C. *Effective Medium Theory: Principles and Application*; Oxford University Press: Oxford, U.K., 1999.
(20) Jeffrey, D. J. *Proc. R. Soc. London, Ser. A: Math., Phys. Eng. Sci.* **1973**, *335*, 355–367.
(21) Batchelor, G. K. *Annu. Rev. Fluid Mech.* **1974**, *6*, 227–255.
(22) Przyluski, J.; Siekierski, M.; Wieczorek, W. *Electrochim. Acta* **1995**, *40*, 2101–2108.
(23) Fredrickson, G. H.; Bicerano, J. *J. Chem. Phys.* **1999**, *110*, 2181–2188.
(24) Merkel, T. C.; Freeman, B. D.; Spontak, R. J.; He, Z.; Pinnau, I.; Meakin, P.; Hill, A. J. *Science* **2002**, *296*, 519–522.
(25) Merkel, T. C.; Freeman, B. D.; Spontak, R. J.; He, Z.; Pinnau, I.; Meakin, P.; Hill, A. J. *Chem. Mater.* **2003**, *15*, 109–123.
(26) Winberg, P.; Eldrup, M.; Maurer, F. H. J. *Polymer* **2004**, *45*, 8253–8264.
(27) Winberg, P.; Desitter, K.; Dotremont, C.; Mullens, S.; Vankelecom, I. F. J.; Maurer, F. H. J. *Macromolecules* **2005**, *38*, 3776–3782.
(28) De Sitter, K.; Winberg, P.; D'Haen, J.; Dotremont, C.; Leysen, R.; Martens, J. A.; Mullens, S.; Maurer, F. H. J.; Vankelecom, I. F. J. *J. Membr. Sci.* **2006**, *278*, 83–91.
(29) Ahn, J. Y.; Chung, W. J.; Pinnau, I.; Guiver, M. D. *J. Membr. Sci.* **2008**, *314*, 123–133.
(30) Choi, B. K.; Shin, K. H. *Solid State Ionics* **1996**, *86−8*, 303–306.
(31) Croce, F.; Appetecchi, G. B.; Persi, L.; Scrosati, B. *Nature* **1998**, *394*, 456–458.
(32) Best, A. S.; Ferry, A.; MacFarlane, D. R.; Forsyth, M. *Solid State Ionics* **1999**, *126*, 269–276.
(33) Forsyth, M.; MacFarlane, D. R.; Best, A.; Adebahr, J.; Jacobsson, P.; Hill, A. J. *Solid State Ionics* **2002**, *147*, 203–211.
(34) Capiglia, C.; Mustarelli, P.; Quartarone, E.; Tomasi, C.; Magistris, A. *Solid State Ionics* **1999**, *118*, 73–79.
(35) Surve, M.; Pryamitsyn, V.; Ganesan, V. *J. Chem. Phys.* **2005**, *122*, 154901.

(36) Surve, M.; Pryamitsyn, V.; Ganesan, V. *Langmuir* **2006**, *22*, 969–981.
(37) Ganesan, V.; Khounlavong, L.; Pryamitsyn, V. *Phys. Rev. E* **2008**, *78*, 051804.
(38) Kropka, J. M.; Pryamitsyn, V.; Ganesan, V. *Phys. Rev. Lett.* **2008**, *101*, 075702.
(39) Khounlavong, L.; Pryamitsyn, V.; Ganesan, V. *J. Chem. Phys.* **2010**, *133*, 144904.
(40) Broutman, L. J.; Agarwal, B. D. *Polym. Eng. Sci.* **1974**, *14*, 581–588.
(41) Moore, T. T.; Mahajan, R.; Vu, D. Q.; Koros, W. J. *AIChE J.* **2004**, *50*, 311–321.
(42) Odegard, G. M.; Clancy, T. C.; Gates, T. S. *Polymer* **2005**, *46*, 553–562.
(43) Xue, L. P.; Borodin, O.; Smith, G. D. *J. Membr. Sci.* **2006**, *286*, 293–300.
(44) Hill, R. J. *Ind. Eng. Chem. Res.* **2006**, *45*, 6890–6898.
(45) Khounlavong, L.; Ganesan, V. *J. Chem. Phys.* **2009**, *130*, 104901.
(46) Jones, R. A. L. *Curr. Opin. Colloid Interface Sci.* **1999**, *4*, 153–158.
(47) Priestley, R. D.; Ellison, C. J.; Broadbelt, L. J.; Torkelson, J. M. *Science* **2005**, *309*, 456–459.
(48) Ellison, C. J.; Torkelson, J. M. *Nat. Mater.* **2003**, *2*, 695–700.
(49) Harms, S.; Ratzke, K.; Faupel, F.; Schneider, G. J.; Willner, L.; Richter, D. *Macromolecules* **2010**, *43*, 10505–10511.
(50) Croce, F.; Curini, R.; Martinelli, A.; Persi, L.; Ronci, F.; Scrosati, B.; Caminiti, R. *J. Phys. Chem. B* **1999**, *103*, 10632–10638.
(51) Croce, F.; Sacchetti, S.; Scrosati, B. *J. Power Sources* **2006**, *161*, 560–564.
(52) Wieczorek, W. *Mat. Sci. Eng. B: Solid State Mater. Adv. Technol.* **1992**, *15*, 108–114.
(53) Boyd, R. H.; Pant, P. V. K. *Macromolecules* **1991**, *24*, 6325–6331.
(54) Gusev, A. A.; Suter, U. W. *J. Chem. Phys.* **1993**, *99*, 2228–2234.
(55) Gusev, A. A.; Arizzi, S.; Suter, U. W.; Moll, D. J. *J. Chem. Phys.* **1993**, *99*, 2221–2227.
(56) Pant, P. V. K.; Boyd, R. H. *Macromolecules* **1993**, *26*, 679–686.
(57) Gee, R. H.; Boyd, R. H. *Polymer* **1995**, *36*, 1435–1440.
(58) Arnould, D.; Laurence, R. L. *Ind. Eng. Chem. Res.* **1992**, *31*, 218–228.
(59) Cicerone, M. T.; Blackburn, F. R.; Ediger, M. D. *Macromolecules* **1995**, *28*, 8224–8232.
(60) Ehlich, D.; Sillescu, H. *Macromolecules* **1990**, *23*, 1600–1610.
(61) Killis, A.; Lenest, J. F.; Gandini, A.; Cheradame, H. *J. Polym. Sci., Part B: Polym. Phys.* **1981**, *19*, 1073–1080.
(62) Ratner, M. A.; Shriver, D. F. *Chem. Rev.* **1988**, *88*, 109–124.
(63) Carmesin, I.; Kremer, K. *Macromolecules* **1988**, *21*, 2819–2823.
(64) Deutsch, H. P.; Binder, K. *J. Chem. Phys.* **1991**, *94*, 2294–2304.
(65) Muller, M.; Binder, K. *Macromolecules* **1995**, *28*, 1825–1834.
(66) Hoffmann, A.; Sommer, J. U.; Blumen, A. *J. Chem. Phys.* **1997**, *106*, 6709–6721.
(67) Weber, H.; Paul, W. *Phys. Rev. E* **1996**, *54*, 3999–4007.
(68) Bortz, A. B.; Kalos, M. H.; Lebowitz, J. L. *J. Comput. Phys.* **1975**, *17*, 10–18.
(69) Chatterjee, A.; Vlachos, D. G. *J. Comput.-Aided Mater. Des.* **2007**, *14*, 253–308.
(70) Fang, S. M. *Chem. Eng. Sci.* **1975**, *30*, 773–780.
(71) Vrentas, J. S.; Duda, J. L. *Macromolecules* **1976**, *9*, 785–790.
(72) Bedrov, D.; Smith, G. D.; Smith, J. S. *J. Chem. Phys.* **2003**, *119*, 10438–10447.
(73) Hooper, J. B.; Schweizer, K. S.; Desai, T. G.; Koshy, R.; Keblinski, P. *J. Chem. Phys.* **2004**, *121*, 6986–6997.
(74) Harrison, A. K.; Zwanzig, R. *Phys. Rev. A* **1985**, *32*, 1072–1075.
(75) Druger, S. D.; Ratner, M. A.; Nitzan, A. *Phys. Rev. B* **1985**, *31*, 3939–3947.
(76) Grankek, R.; Nitzan, A.; Druger, S. D.; Ratner, M. A. *Solid State Ionics* **1988**, *28*, 120–128.
(77) Granek, R.; Nitzan, A. *J. Chem. Phys.* **1990**, *93*, 5918–5934.
(78) Granek, R.; Nitzan, A. *J. Chem. Phys.* **1990**, *92*, 1329–1338.
(79) Nitzan, A.; Ratner, M. A. *J. Phys. Chem.* **1994**, *98*, 1765–1775.
(80) Mullerplathe, F. *J. Chem. Phys.* **1991**, *94*, 3192–3199.
(81) Wang, C. Y.; Ediger, M. D. *J. Phys. Chem. B* **2000**, *104*, 1724–1728.
(82) Caronna, C.; Chushkin, Y.; Madsen, A.; Cupane, A. *Phys. Rev. Lett.* **2008**, *100*, 055702.
(83) Cherdhirankorn, T.; Harmandaris, V.; Juhari, A.; Voudouris, P.; Fytas, G.; Kremer, K.; Koynov, K. *Macromolecules* **2009**, *42*, 4858–4866.
(84) Kob, W.; Donati, C.; Plimpton, S. J.; Poole, P. H.; Glotzer, S. C. *Phys. Rev. Lett.* **1997**, *79*, 2827–2830.
(85) Kasper, A.; Bartsch, E.; Sillescu, H. *Langmuir* **1998**, *14*, 5004–5010.
(86) Kegel, W. K.; van Blaaderen, A. *Science* **2000**, *287*, 290–293.
(87) Torquato, S.; Avellaneda, M. *J. Chem. Phys.* **1991**, *95*, 6477–6489.
(88) Torquato, S. *Random Heterogeneous Materials: Microstructure and Macroscopic Properties*; Springer: New York, 2002.
(89) For instance, the nonbonded polystyrene monomer fullerene interaction has a well depth of between approximately 0.15 and 0.08 kcal/mol in atomistic models.